



**QUEEN'S
UNIVERSITY
BELFAST**

Visualizing Big Energy Data: Solutions for This Crucial Component of Data Analysis

Hyndman, R. J., Liu, X. A., & Pinson, P. (2018). Visualizing Big Energy Data: Solutions for This Crucial Component of Data Analysis. *IEEE Power & Energy Magazine*, 16(3), 18-25.
<https://doi.org/10.1109/MPE.2018.2801441>

Published in:
IEEE Power & Energy Magazine

Document Version:
Peer reviewed version

Queen's University Belfast - Research Portal:
[Link to publication record in Queen's University Belfast Research Portal](#)

Publisher rights
© 2018 IEEE.

This work is made available online in accordance with the publisher's policies. Please refer to any applicable terms of use of the publisher.

General rights

Copyright for the publications made accessible via the Queen's University Belfast Research Portal is retained by the author(s) and / or other copyright owners and it is a condition of accessing these publications that users recognise and abide by the legal requirements associated with these rights.

Take down policy

The Research Portal is Queen's institutional repository that provides access to Queen's research output. Every effort has been made to ensure that content in the Research Portal does not infringe any person's rights, or applicable UK laws. If you discover content in the Research Portal that you believe breaches copyright or violates any law, please contact openaccess@qub.ac.uk.

Visualizing Big Energy Data

Rob J Hyndman, Xueqin Liu and Pierre Pinson

Visualization is a crucial component of data analysis. It is always a good idea to plot the data before fitting any models, making any predictions, or drawing any conclusions. As sensors of the electric grid are collecting large volumes of data from various sources, power industry professionals are facing the challenge of visualizing such data in a timely fashion. In this article, we demonstrate several data visualization solutions for big energy data through three case studies involving smart meter data, phasor measurement unit (PMU) data, and probabilistic forecasts, respectively.

1. Visualizing Smart Meter Data

Smart grid initiatives worldwide have deployed millions of smart meters to the electric grid. A small to medium sized utility company could have thousands of meters spread across its territory, recording electricity demand at hourly or sub-hourly intervals. But how should one actually plot data on thousands of smart meters, each comprising thousands of observations over time? We cannot simply produce time plots of the demand recorded at each meter, due to the sheer volume of data involved.

One approach is to convert each long series of demand data to a single two-dimensional point which can be plotted in a simple scatterplot. In that way, all the meters can be seen in the scatterplot; so outliers can be detected, clustering can be observed, and any other interesting structure can be examined. In this section, we will present a solution to this problem by first converting the data from each smart meter into series of probability distributions, which are then used to compute pairwise distances between load profiles. Finally, the households are embedded in two-dimensional space to enable simple but informative plots to be constructed.

Irish smart meter data

To illustrate, we will use data collected during a smart metering trial conducted by the Commission for Energy Regulation (CER) in Ireland. For demonstration purposes, we will use measurements of half-hourly electricity consumption gathered from 500 residential consumers over 535 consecutive days. Every meter provides the electricity consumption between July 14th, 2009 and December 31st, 2010. Many of the series have periods of missing data. The CER data set does not account for energy consumed by heating and cooling systems. Either the households use a different source of energy for heating, such as oil and gas, or a separate meter is used to measure the consumption due to heating. Further, no installed cooling system has been reported in the study.

Data from two smart meters are shown as simple time series plots in Figure 1. While it is obvious that these meters have very different demand patterns, it is not possible to say much more — the time of day and day of week patterns are hidden due to the volume of data, and even the median demand is not clear from such plots.

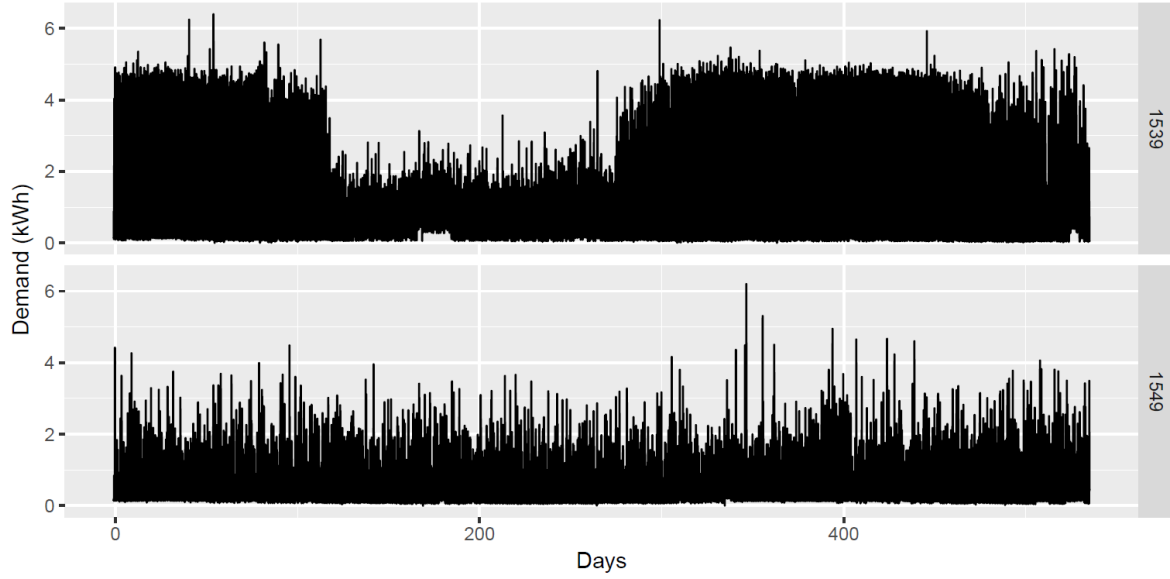


Figure 1: Two examples of smart meter demand from the CER data set.

Percentiles by time of week

One way to see intra-day and intra-week patterns, is to plot the demand against the time of the week, rather than against the time since the beginning of data collection. Figure 2 shows the same data as were displayed in Figure 1, but as a scatterplot against the time of the week. Now, the morning and evening peaks for meter 1539 become clear, and it also becomes apparent that meter 1549 has a different pattern on weekends than on weekdays.

To further look into the intra-day load profiles, we can leverage the concept of percentile, which describes the distribution of the observations. The 10th percentile, for example, is the value below which 10% of the observations may be found. Widespread percentiles indicate widespread observations. On the other hand, depending upon the thickness of the percentiles on a plot, they may be overlapping each other, which indicate that the observations are close to each other. In the extreme case where all observations are identical, the percentiles are identical too.

Overlaid on the individual demand data, Figure 2 also shows some percentiles of the demand distributions as they vary by half-hour and day of the week, allowing us to see $48 \times 7 = 336$ probability distributions per household. For some periods, such as early morning around 4 am for meter 1549, the selected percentiles are indistinguishable, indicating similar load levels. This is because electricity consumption activities during sleeping hours is low and relatively certain. The evening hours (e.g., hours 18 to 24) are showing widespread percentiles, as the result of varying electricity consumption activities.

The percentiles are smoothed a little over time, by combining neighboring half-hours. For example, the percentiles for half-hour h are estimated using the data for half-hours $h - 1, h, h + 1$. This is equivalent to a form of kernel smoothing across half-hours. We use a simple estimate of each percentile to compute these curves. In this context, simple estimates are better than kernel density estimates (or some other more sophisticated estimate of the distribution) because the data set contains a large number of zeros, making the distribution a mixture of a discrete component and a continuous component. Also, the high skewness of the data, and the non-negative nature of demand, makes it problematic to use kernel density estimates.

There are several advantages in working with the percentiles rather than the data directly. It avoids problems with missing observations, and with the specific timing of household events (e.g., parties), and focuses attention on typical behavior of a household throughout the week. Although only five percentiles are shown in Figure 2, we actually compute percentiles for probabilities 1, 2, \dots , 99%.

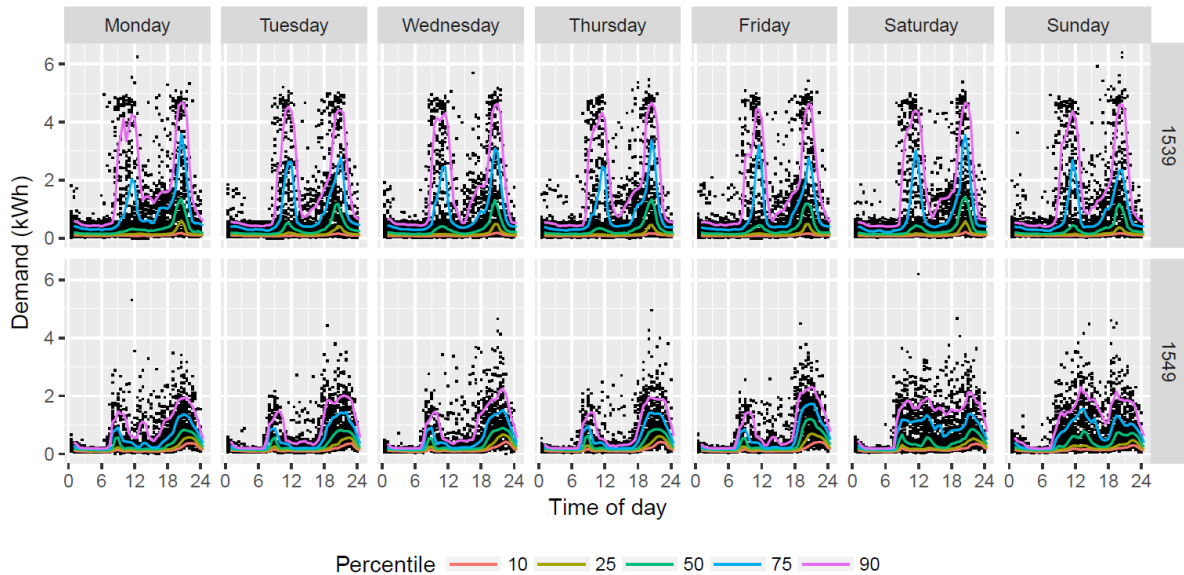


Figure 2: Demand plotted against time of the week for two smart meters from the CER data set.

Typical and anomalous households

In order to study the whole group of household demand distributions, we will first compute the differences in electricity consumption patterns between pairs of households. Statistically speaking, we call these differences “distances”. Note that the “distance” used in this section refer to the distance between two probability distributions rather than the physical distance between two houses. One way to measure the distance between two distributions is the Jensen–Shannon divergence. We have 336 probability distributions per household, one for each half-hour period of the week, so we have 336 Jensen–Shannon distance measures for each pair of households. We can measure the overall distance between the distributions from two households by summing these 336 Jensen–Shannon distance measures. In this way, we can find the distance between each pair of households in the data set.

From these pairwise distances, we can compute a measure of the “typicality” of a specific household, by seeing how many similar houses are nearby according to Jensen–Shannon divergence. If there are many households with similar probability distributions, the typicality measure will be high. But if there are few similar households, the typicality measure will be low. This gives us a way of finding anomalies in the data set—they are the smart meters corresponding to the least typical households. The most anomalous (i.e., least typical) household is shown in Figure 3. This is clearly a very strange demand distribution, with extremely low demand almost all of the time, reflected by almost overlapping percentiles.

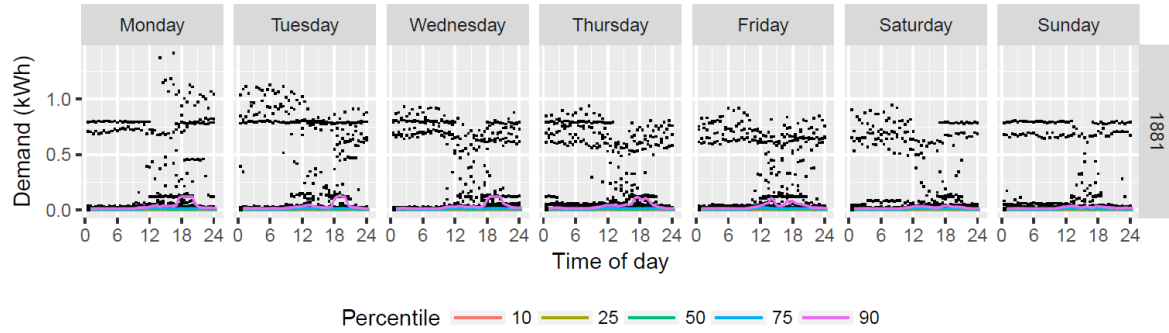


Figure 3: Demand distribution of the least typical household out of the 500 smart meters included in the analysis.

Visualization via embedding

The pairwise distances between households can also be used to create a plot of all households together. If we compute 99 percentiles for 48 half-hours per day and 7 days a week, each of the household distributions can be thought of as a vector in K -dimensional space where $K = 99 \times 48 \times 7 = 33,264$. To easily visualize these, we need to project them onto a two-dimensional space. There are several ways of doing this, such as principal components analysis, multi-dimensional scaling, and so on. The method that we've used here is a "Laplacian eigenmap" to keep the most similar points in K -dimensional space as close as possible in the two-dimensional space.

Figure 4 shows a two-dimensional embedding of the 500 households in this data set. The colors are taken from the measure of typicality, with the most typical 1% of points shown in red, and the least typical 1% of points in black. The remaining points are divided into two groups with all orange points being more typical than the yellow points. The blue numbers show the ranking of anomalous points. The most anomalous point (#1) corresponds to the data shown in Figure 3.

The colors can also be interpreted as corresponding to highest density regions (HDRs) in the original K -dimensional space. This way of plotting the data easily allows us to see the anomalies, to identify any clusters of observations in the data, and to examine any other structure that might exist.

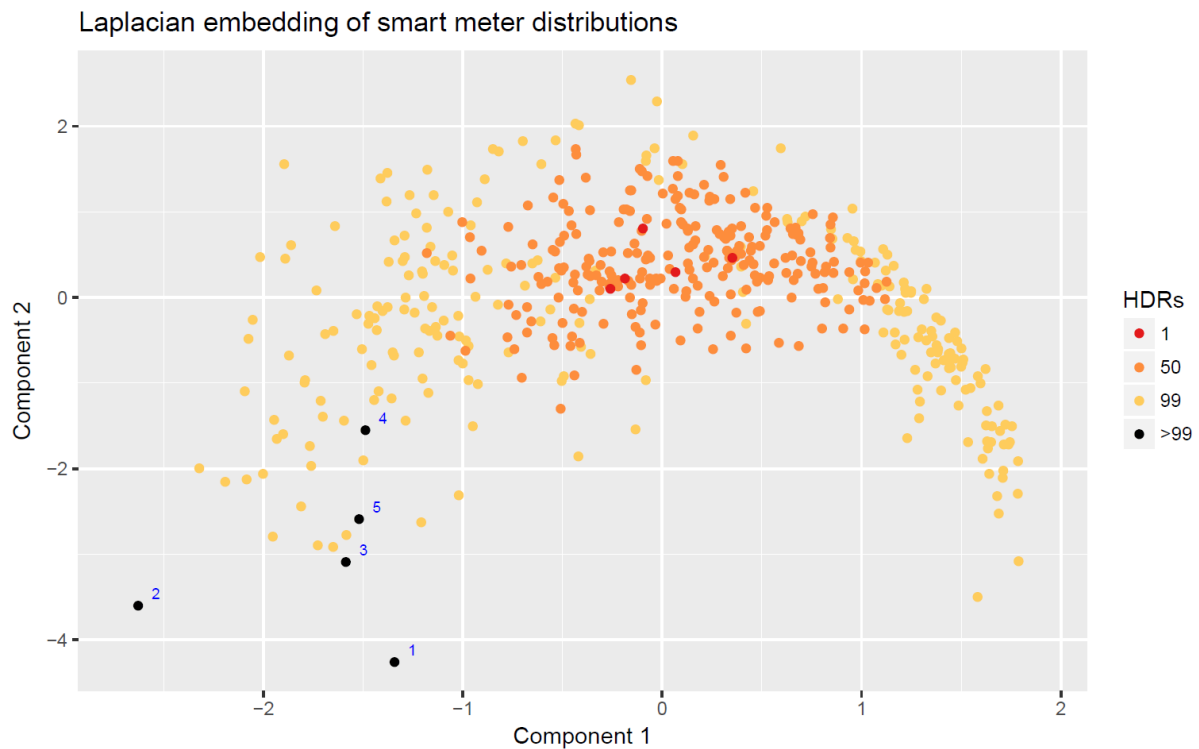


Figure 4: A two-dimensional representation of the data from all 500 households. The most typical points are shown in red, and the most anomalous are shown in black.

2. Visualizing PMU Data

Since the first prototype PMUs were developed by Virginia Tech in 1988, networked PMUs have been rapidly deployed in the last few years. As of early 2016, China and the US have the world's largest PMU networks, each having more than 2000 PMUs in operation. Unlike the existing supervisory control and data acquisition (SCADA) systems which provide measurements every 2 to 4 seconds, PMUs can report data, with accurate and precise time-stamps, 10 to 60 times per second. Consequently, we receive large volumes of high dimensional PMU data continuously, day in and day out. Taking 30 PMUs for example, the system operator needs to manage approximately 15 MB of data per minute, 20 GB per day, 140 GB per week or 7 Terabytes per year. The volume of PMU data will increase dramatically when thousands of PMUs are installed.

The problem of 'too much data, too little information' must be solved – as it is becoming increasingly difficult for the system operator to make use of the raw PMU data for real-time decision making. On the one hand, there is an explosion in the availability of high rate data streams due to advances in monitoring PMU devices, leading to data overload. On the other hand, there is limited understanding on how to extract actionable information from these data-intensive monitoring devices for real-time monitoring and control purposes. "Big-data visual-analytics" offers a way forward, helping to convert these big data streams into actionable insight in real-time, and will aid development of next generation energy management systems. In this section, we will demonstrate the most basic dimension reduction technique, principal component analysis (PCA), as a fundamental tool for the initial steps of visualizing PMU data.

A simple dimension reduction tool – Principal Component Analysis

PCA, first proposed in 1901, is one of the most popular dimension reduction techniques. Using PCA, we can remove the correlation between the variables and select only a few linearly uncorrelated variables to represent the original data. We can view PCA as a form of orthogonal rotation, where the new axes can capture the maximum variance of the data. The orthogonal direction of the maximum variance can be identified by carrying out eigenvalue and eigenvector analysis of the covariance matrix of the sample data, so that the maximum variance corresponds to the largest eigenvalues. The transformed new variables are called the principal components, while the first few principal components can explain most of the variance of the data. Thus we only require a reduced set of them to represent most of the information from the original data.

For event detection and diagnosis purpose, we define two statistics, the T^2 and Q . The T^2 constructed by the principal components, is associated with the PCA model space and represents significant variation of the original data. The Q represents the squared error of the model mismatch and the variation of the data within the residual subspace. Applying PCA on PMU data, we can analyze many sets of measurements from various locations simultaneously. We will demonstrate the elegance and the beauty of PCA through two case studies, selected from the Great Britain and the Irish power networks.

Case 1: Visualizing frequency data to distinguish multiple events in the Great Britain networks

The data used here were recorded from six sites in the Great Britain networks with a 10 Hz sampling rate through the OpenPMU project, including one located in Southern England, one in Manchester and four in Orkney Islands. The well-documented event on September 30th, 2012 saw a loss of load at 02:28 in the morning. Later in the same day a Great Britain - France interconnector trip event at 15:03, resulted in a Great Britain frequency drop from 49.97 to 49.60 Hz in a matter of 10 seconds. The initial rate of change of frequency (RoCoF) activated RoCoF based islanding protection, erroneously disconnecting distributed generation.

We can group data from this single day into four different classes, the normal data, the loss of load, the generation dip, and the islanding event. To visualize this in Figure 5, we have plotted seven days of data randomly selected from two locations to obtain frequency coverage for normal operating conditions. It ranges from 49.8 Hz to 50.2 Hz, represented by the black dots surrounded by the red box – this depicts the 99.9% confidence limit. The normal data from September 30th, 2012 fall in this category. In Figure 5, we have also plotted the loss of load, the generation dip, and the islanding events from two locations. How should we interpret the patterns in this figure? Frequency is the universal parameter of the synchronous power grid, and it possesses simple and elegant characteristics. That is, the frequency data points from two locations are approximately aligned with the $y \approx x$ line. The first principal component t_1 , which captures 99% of the total variance of the frequency data, is thus following this direction. In other words, we can use only one principal component to represent all frequency variables recorded across the grid. In Figure 5, we also notice that the generation dip and loss of load events are in line with the first principal component direction, but outside the red box, with the loss of load sitting at the higher end, and the generation dip sitting at the lower end. When the loss of load and generation dip events occurred in the system, the frequency variables may significantly deviate from the nominal value (50 Hz in this case), but not deviate against each other significantly. However, for the islanding event, it is more likely that the islanded frequency deviates significantly from the rest of the system frequency, and thus is not in line with the principal component direction. That is to say, the islanding data has its projection to the orthogonal direction to t_1 (represented by the Q axis) and is outside the red box. In

comparison to traditional time series graph, the relative relationship of multiple events in comparison to normal operation conditions are much more straightforward, as illustrated in the scatterplot of Figure 5.

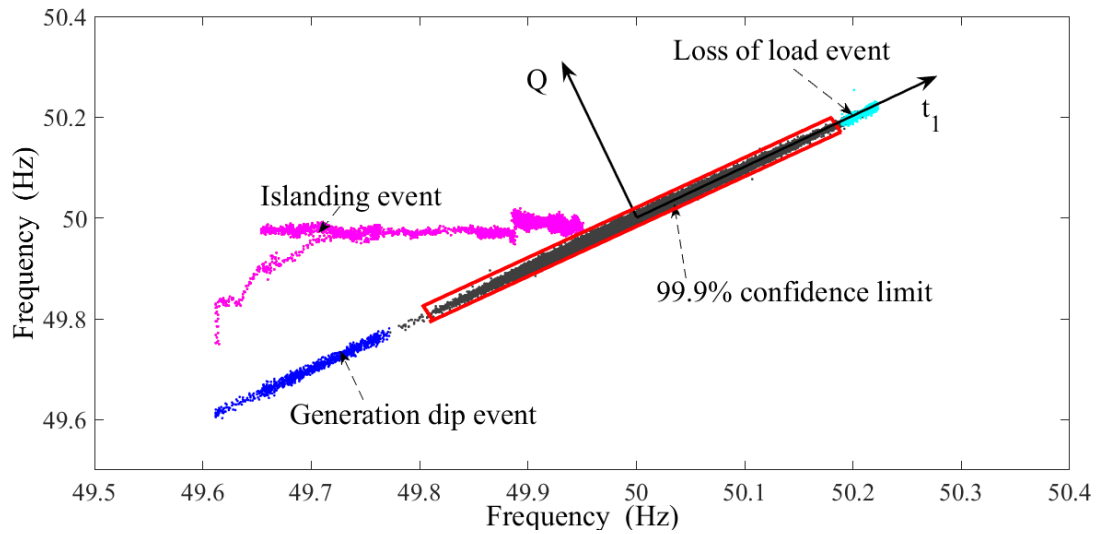


Figure 5. The 2-D illustration for multiple events on September 30th, 2012 recorded in the Great Britain networks. Black, blue, cyan, and purple dots represent the normal data, generation dip, loss of load, and islanding event, respectively.

Once an islanding event is detected in the system, the system operator will try to find out where the event is located. We can accomplish this task by a simple contribution plot to visualize the contribution of individual frequency variables to the pre-defined PCA statistics. If the contribution of a particular frequency variable toward the Q statistic is large, an islanding site can be identified. Figure 6 illustrates variable 5 (representing PMU installed in the Orkney Island, where the islanding occurred) dominates the contribution to Q statistic during the 9 minutes when it happened from 15:03:30 to 15:12:30. Both systems synchronized at 15:12:30.

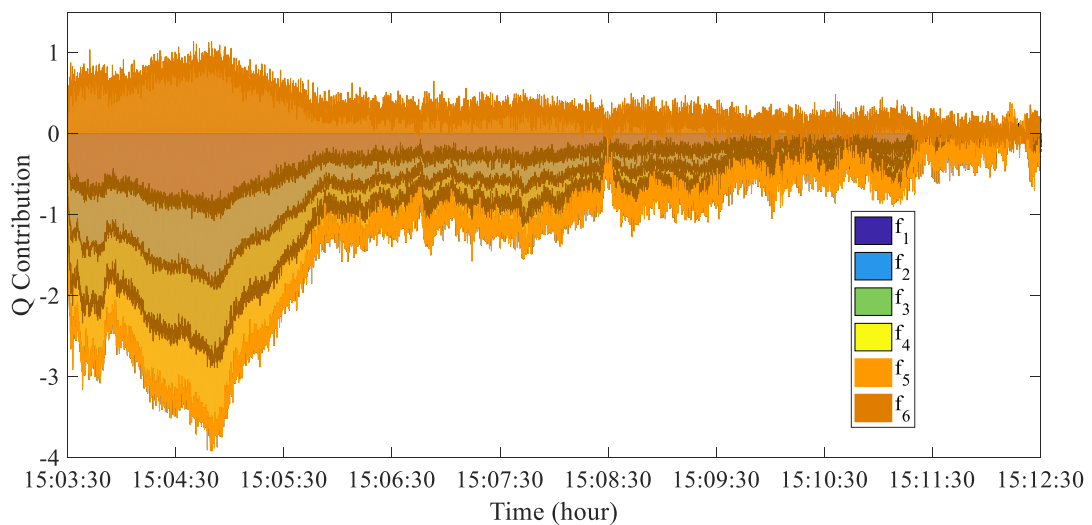


Figure 6. Contribution plot to the Q statistic for case 1.

Case 2: Visualizing post-disturbance voltage data from multiple locations in the Irish networks

We illustrate the post-disturbance voltage trajectory during an East West Interconnector (EWIC) 500MW export trip test event in the Irish network, to further demonstrate PCA as a powerful dimension reduction tool for visualization.

Traditionally the system operator will monitor the voltage traces from various locations. However, it is difficult to manage hundreds of PMUs through this traditional approach. In addition, the interaction among multiple voltage variables embedded in multiple locations is unknown. By applying PCA on the PMU data collected from twenty locations across the network, we found that three principal components are enough to monitor voltages across the entire network. The three selected principal components are capable of explaining 98% of the variance of the data during the test. As illustrated in the scatterplot of the three principal components in Figure 7, the original steady state is represented by the yellow dots, as the event progresses, it goes from the black dots to the red ones and the blue ones, and finally settled to a new steady state represented by the green dots. The spiral trace indicates the oscillatory behavior during this test. The graphical visualization in Figure 7 provides a faster and easier way to interpret information, which helps reduce the decision-making time.

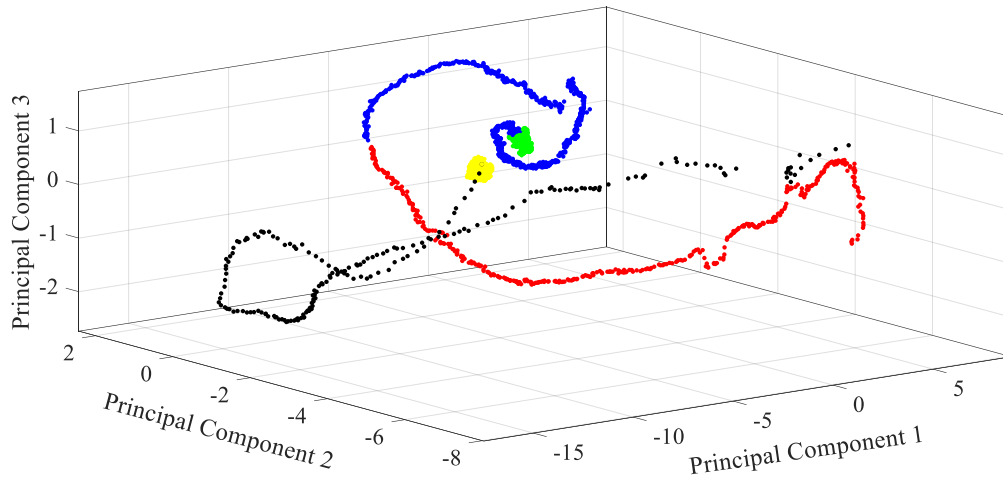


Figure 7. Scatterplot of three principal components of twenty voltage variables recorded in the Irish networks for case 2

3. Visualizing Probabilistic Forecasts

While visualizing the data at the beginning of data analysis is well-known to be a must-have step, visualizing the results from sophisticated models is equally important. Here we will present another case study, focusing on the visualization of forecasting results. Specifically we will use wind power forecasts as an example, although the methodology can be generally applied to other energy forecasts, such as solar power forecasts and load forecasts.

Uncertainty has always been around in power system operation and planning. For example, operational decision and control problem uncertainties originate from contingencies (generation units and lines), incomplete or erroneous overview of the system state, and projections of future demand. Today however, with the rapid deployment of renewable energy generation capacities throughout the world, new uncertainties are appearing that directly relate to how much power may be generated in the following minutes, hours, days, and beyond. Similarly on the electricity consumption side, uncertainties are growing, due to changes in consumption patterns (electric vehicles, more proactive consumers, etc.), but also to behind-the-meter power generation. All in all, combined with an all-time high availability of relevant data, this has supported the increased focus on developing new approaches to analytics and forecasting for power system operations and control.

While traditional point (or single-valued) forecasts can provide the expected values for the variable of interest, probabilistic forecasts, which have now been around for more than a decade, can further quantify the future uncertainties via quantiles, intervals, or probability distributions. Nevertheless, it is challenging to visualize such uncertainties, so that the probabilistic forecasts can be effectively communicated to and ultimately accepted by the business consumers of these forecasts. In this section, we will introduce and discuss alternative approaches to visualizing probabilistic wind power forecasts.

“River-of-blood” fan chart

A prominent example of communicating probabilistic forecast information is through a “river-of-blood” fan chart as depicted in Figure 8. An earlier version of it was used in a significant number of technical presentations and broad-audience articles to introduce and illustrate the concept of probabilistic wind power forecasting since 2005. This plot aims at illustrating hourly power generation from wind power (in this case, for the whole wind power generation of western Denmark), with an hourly resolution up to nearly two days ahead. This visualization proposal is inspired by the Bank of England probabilistic forecasts for inflation, published on a quarterly basis from 1996, comforting it as a pragmatic and intuitive approach to convey uncertainty information.

This so-called “river-of-blood” fan chart associates the traditional single-valued forecasts, telling about the mean of potential renewable power generation in the near future (formally, the conditional expectation), with a number of prediction intervals. These prediction intervals have an increasing nominal coverage rate, hence intuitively getting wider for lighter colors. For a given lead time, a prediction interval gives a range within which power generation may lie, given a certain a-priori probability, i.e., its nominal coverage rate. Those prediction intervals are centered in probability on the median. The interest of that visualization is that it appeals to both a broad audience and expert practitioners. The former may be content with a simple and intuitive way to see how uncertain the forecasts are, while the latter is actually provided with enough information to reconstruct full predictive densities to be used as input to a wide range of decision and control problems in a stochastic optimization framework. Note that Figure 8 does not mean to show accurate wind power forecasts, so readers may ignore the fact that many observations are falling outside the 90% prediction interval.

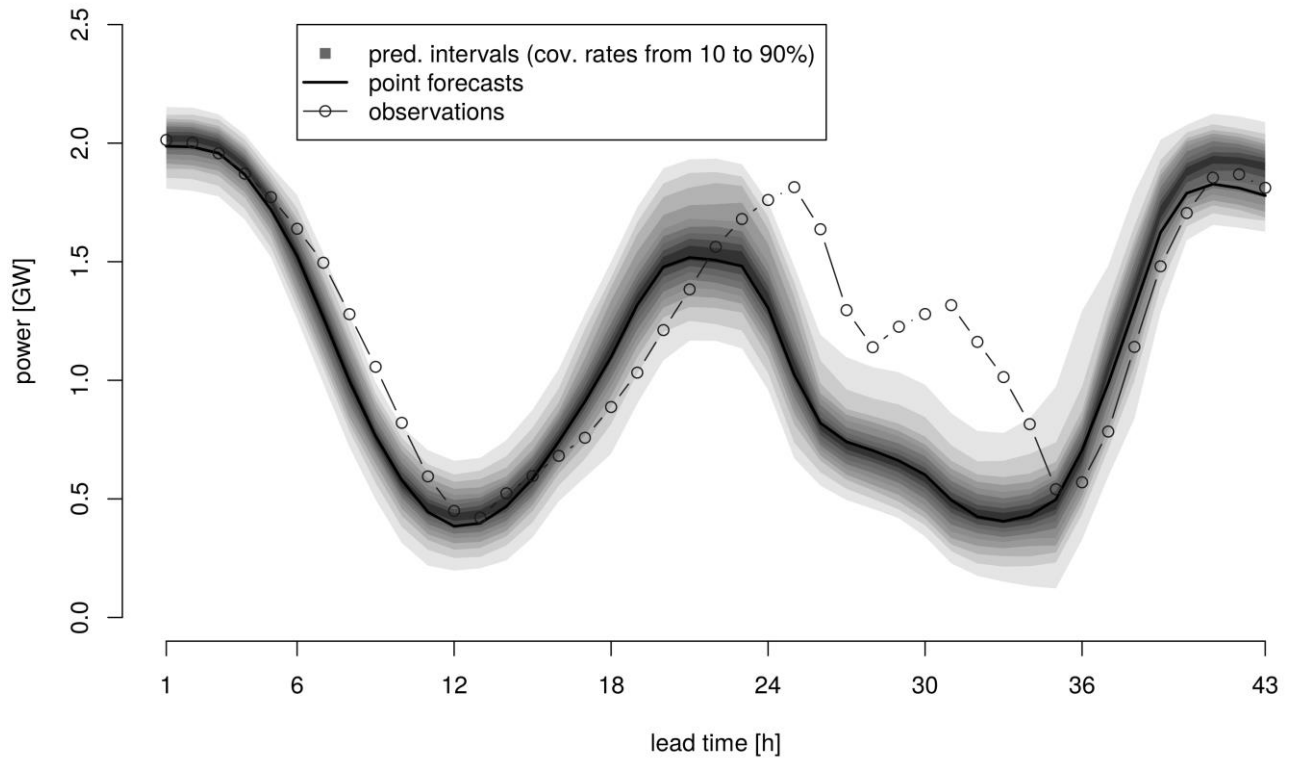


Figure 8. Probabilistic forecasts represented as a river-of-blood fan chart, with decreasing shade intensity for higher nominal coverage rate of the prediction intervals, for the whole wind power generation of western Denmark, with an hourly resolution up to nearly two days ahead.

Ensemble forecasts

While the visualization in Figure 8 is appealing, it is not the only way to communicate probabilistic forecast information. Indeed, instead of focusing on how uncertain the future may or may not be, an alternative approach aims at providing the forecast user with a set of alternative trajectories in the future. This approach was championed by the meteorological community, which coined the term of ‘ensemble forecast’ for it. In practice, this has translated to a number of high value applications, for instance related to trajectories of storms and cyclones and their potential impact.

For the case of renewable energy generation, this type of representation has attracted increased interest due to the additional information it conveys, also allowing the use of these alternative futures as input to existing tools for operations and control within a deterministic framework. As an example, Figure 9 depicts the ensemble forecasts that are used to convey the probabilistic forecast information for Western Denmark, for a given day in the past. Since they are based on related methods, the general probabilistic information shown in Figures 8 and 9 has similarities, especially in terms of trends and uncertainty levels. However, the ensemble forecasts in Figure 9 provide an additional information in terms of dependencies among lead times, which is not conveyed by river-of-blood fan charts.

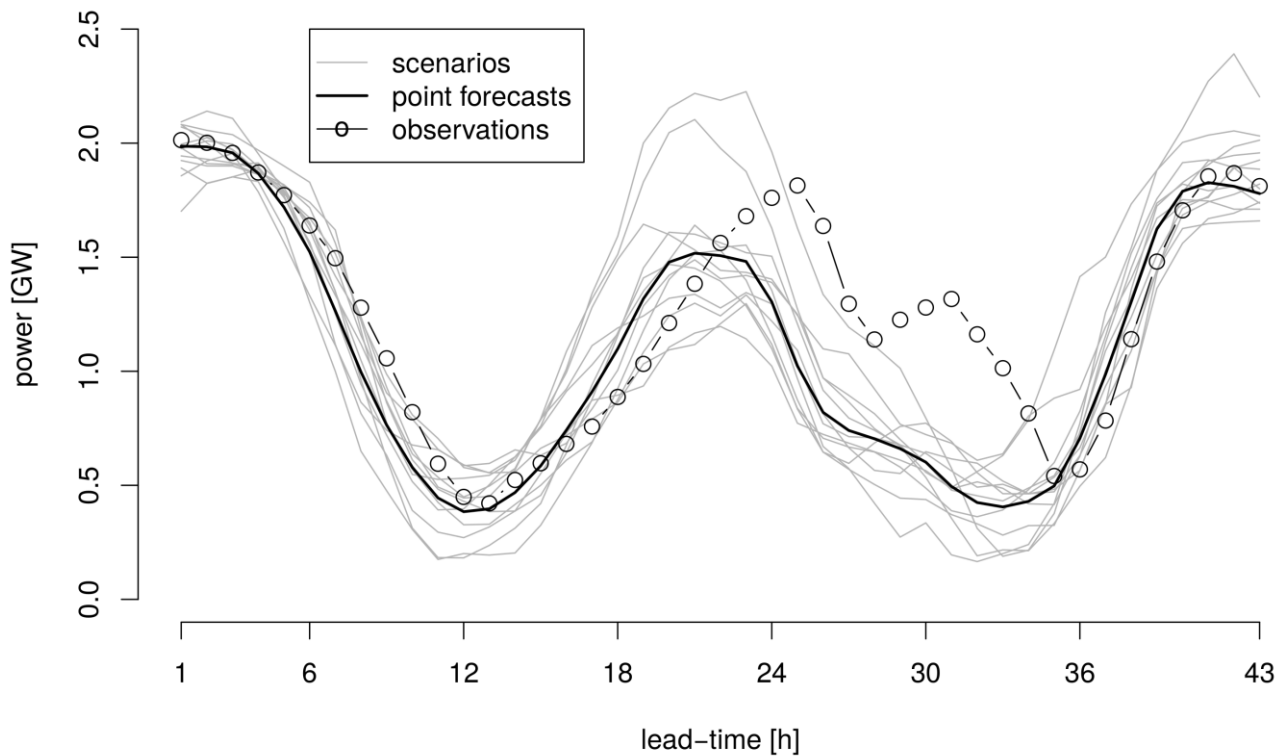


Figure 9. Probabilistic forecast information conveyed by ensemble forecasts for the whole wind power generation of western Denmark.

Concluding Remarks

In this article, we have offered a few examples of visualizing big energy data. Although these examples spread across distribution (smart meter data), transmission (PMU data) and generation (wind power forecast data), and cover both pre-modeling and post-modeling stages, the paper does not attempt to be comprehensive. There are many other insightful plots we are not able to present due to page limitation, such as maps for geospatial information (e.g., load growth and penetration of electric vehicles). Moreover, some insights are better presented dynamically via animation rather than on a static paper, such as changes of load and temperature relationship over time, and customer behavior changes due to the adoption of demand response programs. We hope that this article can inspire more and more researchers and practitioners to create effective plots from energy data.

Further Readings

Belkin, M and P Niyogi (2003). Laplacian Eigenmaps for Dimensionality Reduction and Data Representation. *Neural Computation* 15(6), 1373–1396.

Hyndman, RJ and Y Fan (1996). Sample quantiles in statistical packages. *The American Statistician* 50(4), 361–365.

X. Liu, D. Lavery, R. Best, K. Li, D.J. Morrow and S. McLoone (2015), “Principal Component Analysis of Wide Area Phasor Measurements for Islanding Detection - A Geometric View,” *IEEE Trans. Power Del.*, 30(2), 976–985.

X. Liu, J. Kennedy, D. Lavery, D. Morrow, S. McLoone (2016), “Wide Area Phase Angle Measurements for Islanding Detection - An Adaptive Nonlinear Approach”, *IEEE Trans. Power Del.*, 31(4), 1901-1911.

Juan Miguel Morales, Antonio Conejo, Henrik Madsen, Pierre Pinson, Marco Zugno (2014). *Integrating Renewable in Electricity Markets – Operational Problems*. Springer Verlag, Int. Series in Operational Research & Management Science.

Ricardo Bessa, Corinna Möhrle, Vanessa Fundel, Malte Siefert, Jethro Browell Sebastian Haglund El Gaidi, Bri-Mathias Hodge, Umit Cali, George Kariniotakis (2017). Towards Improved Understanding of the Applicability of Uncertainty Forecasts in the Electric Power Industry. *Energies* 10(9), 1402.

Bio

Rob J Hyndman is a Professor of Statistics at Monash Business School, and Editor-in-Chief of the *International Journal of Forecasting*.

Xueqin (Amy) Liu is a Lecturer of Smart Grid Data Analytics at Queen’s University Belfast, UK.

Pierre Pinson is a Professor of Electrical Engineering and Head of the Energy Analytics & Markets group at the Technical University of Denmark.